EurJIC
European Journal of Inorganic Chemistry

Full Papers
doi.org/10.1002/ejic.202100042

Chemistry Europe
European Chemical Societies Publishing

Special Collection

Immobilized Ru-Pincer Complexes for Continuous Gas-Phase Low-Temperature Methanol Reforming-Improving the Activity by a Second Ru-Complex and Variation of Hydroxide Additives

Christian H. Schwarz,[a] Dominik Kraus,[a] Elisabetta Alberico,[b, c] Henrik Junge,[b] and Marco Haumann*[a]

Ru-pincer complexes were immobilized as supported liquid phase (SLP) materials to allow the methanol reforming reaction as continuous gas phase process. Under reaction conditions, the liquid phase forms from the hydroxide coating. Several hydroxides were screened and CsOH showed highest activity compared to the standard KOH coating. The well-known Ru-pincer complex carbonylchlorohydrido [bis(2-di-i-propylphosphinoethyl)amine]ruthenium(II) is limited in catalyzing the final step of the methanol reforming. Addition of a second complex, having a methylated backbone in the pincer-ligand, could overcome these limitations. Significant enhancement of the overall catalytic activity was observed.

Introduction

Renewable energies like wind and solar are subject to temporal fluctuation and efficient storage of the excess energy is mandatory for an efficient green energy scenario.[1] Excess energy can be stored in form of batteries, by converting electrical energy into other forms of energy (e.g. by means of a pumped storage power station) or by producing a chemical energy carrier. Hydrogen, for example, can be used as a suitable chemical energy carrier.[2] Its generation by electrolysis and conversion in fuel cells are established technologies along the process chain.[3,4] However, storing pure hydrogen is challenging, given the low volumetric storage capacity.[5] In recent years, storage of hydrogen in chemical form by catalytic hydrogenation of organic molecules, so called liquid organic hydrogen carriers (LOHC), became an interesting alternative.[6–13] From LOHC materials, hydrogen can be liberated by dehydrogenation catalysis. Today, hydrogen storage materials range from simple NH_3 to more complex structures like dibenzyltoluene. A promising approach to hydrogen storage is the generation of methanol by hydrogenation of CO_2.[14] Methanol has the advantage of a relatively high hydrogen content of 12.5 wt% in the molecule. In addition, methanol is liquid under ambient conditions and can be stored in tanks without modifications of the existing infrastructure. In a decentralized scenario, even for mobile applications in transport, the hydrogen can be released again by methanol steam reforming.[15] The resulting reformate has a hydrogen to carbon dioxide product ratio of 3:1 according to Scheme 1.

From a thermodynamic point of view, high equilibrium conversions of reaction (R1) can be obtained at higher temperatures since the reaction is endothermic. However, in case the reaction temperatures exceed approx. 200 °C, the stronger endothermic methanol decomposition (R2) will result in high CO levels >1%, which would render the gas mixture not suitable for most fuel cell applications.[16,17] Since CO is converted in the presence of water via reaction (R3), lower reaction temperatures will lead to higher hydrogen purity. Heterogeneous catalysts, however, will drastically lose activity at such temperatures, making the process not feasible from a kinetic point of view.[17,18]

In recent years, a wide range of homogeneous catalysts has successfully been employed in the field of low temperature aqueous phase methanol reforming (AMR).[19–23] These catalysts, some of which are shown in Figure 1, facilitate the release of hydrogen with carbon dioxide as a by-product from methanol and water at temperatures below 100 °C. Hence, the CO contamination level can be as low as <1 ppm. One of the most promising catalyst systems, which combines high productivity (turnover number >350,000), good long term stability (> 3 weeks) and low concentrations of carbon monoxide as side product (<10 ppm) is the ruthenium-based PNP-pincer catalyst **3** published by Beller and co-workers.[24] Base metal homogeneous catalysts with similar pincer motifs (see e.g. **4**) have also

[a] C. H. Schwarz, D. Kraus, Dr. M. Haumann
Friedrich-Alexander-Universität Erlangen-Nürnberg (FAU), Lehrstuhl für Chemische Reaktionstechnik (CRT),
Egerlandstr. 3, 91058 Erlangen, Germany
E-mail: marco.haumann@fau.de
https://www.crt.tf.fau.de/
[b] Dr. E. Alberico, Dr. H. Junge
Leibniz-Institut für Katalyse, e. V.,
Albert-Einstein Straße 29a, 18059 Rostock, Germany
[c] Dr. E. Alberico
Istituto di Chimica Biomolecolare, Consiglio Nazionale delle Ricerche,
tr. La Crucca 3, 07100 Sassari, Italy

Supporting information for this article is available on the WWW under https://doi.org/10.1002/ejic.202100042

Special Collection Part of the Supported Catalysts Special Collection.

$$CH_3OH + H_2O \rightleftharpoons 3\,H_2 + CO_2 \quad \Delta H = 49.6\ kJ\ mol^{-1} \quad (R1)$$

$$CH_3OH \rightleftharpoons 2\,H_2 + CO \quad \Delta H = 90.8\ kJ\ mol^{-1} \quad (R2)$$

$$CO + H_2O \rightleftharpoons H_2 + CO_2 \quad \Delta H = -41.3\ kJ\ mol^{-1} \quad (R3)$$

Scheme 1. Reaction network of methanol reforming including the side reaction (R2) leading to CO formation and the water-gas shift reaction (R3).

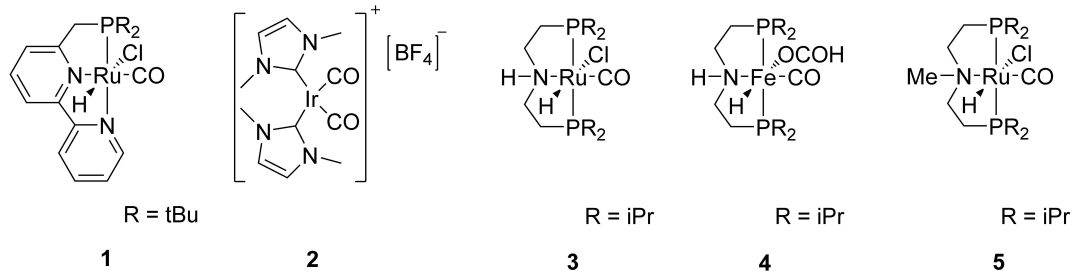

Figure 1. Selected examples of transition metal complexes reported for the aqueous phase methanol reforming.

been investigated. However, such catalysts were not as active as the ruthenium-based system and suffered from a high oxygen sensitivity.

From a mechanistic point of view, the AMR reaction proceeds in three steps via formaldehyde and formic acid to finally yield a product composition of carbon dioxide and hydrogen in a ratio of 1:3. When only complex **3** is applied, the rate determining step of the reaction sequence was found to be the final dehydrogenation of formate (step 3 in Scheme 2), resulting in the accumulation of formate during the reaction.[25] By screening for a second catalyst to lower the activation barrier of this step, Beller and co-workers were able to improve the dehydrogenation of formate.[26]

The best complex was based on a simple modification in the backbone of the PNP-pincer ligand, indicated by structure **5** in Figure 1. Although the structures of complexes **3** and **5** are very similar, their catalytic properties differ significantly. The rate determining step of **5** is the dehydrogenation of methanol to formaldehyde (step 1 in Scheme 2). The fact that both complexes accelerate the rate determining step of their counterpart is utilized in the bi-catalytic system with a 1:1 molar ratio of **3:5** to reach higher turn-over frequencies (TOF) by up to 50% compared to the use of **3** alone. Furthermore, the absolute amount of base could be reduced to 12.5% compared to initial studies using 80 mmol KOH.

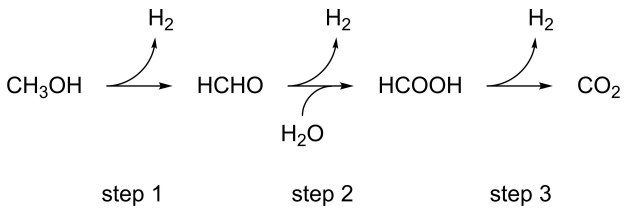

Scheme 2. Proposed reaction sequence for methanol reforming.

In our previous work complex **3** was successfully immobilized using the supported liquid phase (SLP) concept.[27] Here, the homogenous complex **3** is entrapped in a thin film of KOH, which is liquid under reaction conditions due to dissolved amounts of water and methanol. This aqueous KOH film is dispersed over the large inner surface area of a porous support material, in this case alumina. These SLP catalysts were then employed in a continuous vapor-phase methanol steam reforming process (MSR). KOH is required for catalytic activity as well as catalyst complex activation. Dissolving 2 wt% of complex **3** in 10 wt.–% of KOH on porous alumina allowed reasonable activity of 14 $mol_{H2}\,mol_{Ru}^{-1}\,h^{-1}$ (short h^{-1}) and a high selectivity of 99.0% CO_2 (corresponding to less than 2500 ppm CO) at 150 °C and 1 bar. More important for continuous processes, the stability of the catalyst was maintained over 70 h time on stream (TOS) with minor deactivation. Due to the crucial role of the base additive for catalyst performance, we became interested in investigating the influence of different base additives for gas-phase methanol reforming. In addition, we employed the combination of complexes **3** and **5**, the so-called bi-catalytic system, in order to investigate the impact of complex **5** on overall performance.

Results and Discussion

In a first series of experiments we investigated different alkali metal hydroxides as basic additives for the MSR catalyst. The

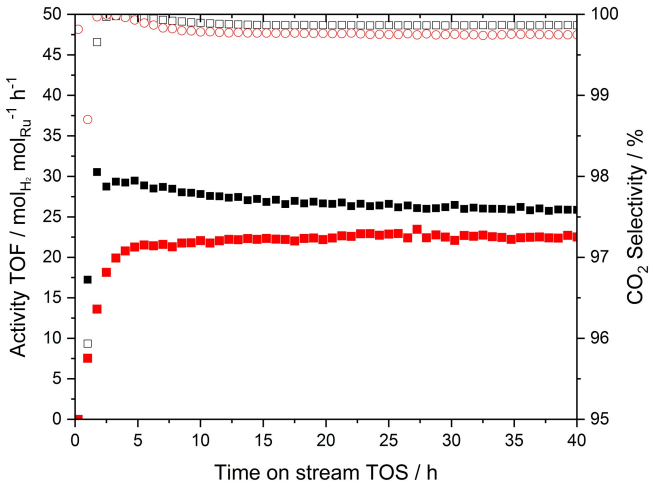

Figure 2. Activity (filled symbols) and CO_2 selectivity (open symbols) over time on stream for methanol reforming using Ru-**3**-SLP catalysts with different hydroxide coatings of KOH (black squares) and CsOH (red circles). Reaction conditions: p_{abs}: 1 bar; $p_{MeOH|H2O}$: 0.5 bar; T: 150 °C; m_{SLP}: 5.0 g; Q_{tot}: 50 ml min^{-1}. Catalyst composition: 50 µmol$_{Ru}$ g$_{Support}^{-1}$; 10 wt% MOH-loading; Aluminum oxide support material 1.0 mm Ø.

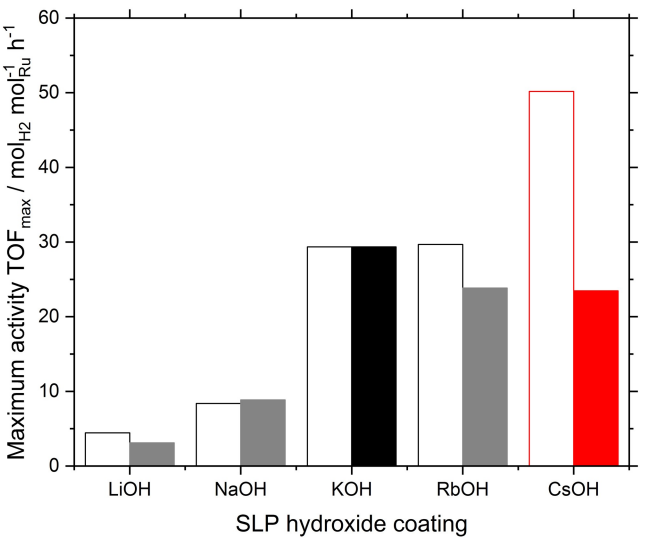

Figure 3. Maximum activity (TOF_{max}) of immobilized Ru-**3**-SLP catalysts in continuous methanol reforming with different alkali hydroxides and different loadings. Reaction conditions: T = 150 °C, p_{abs}: 1 bar; $p_{MeOH|H2O}$: 0.5 bar; m_{SLP}: 5.0 g; Q_{tot}: 50 ml min^{-1}. Catalyst composition: 50 µmol$_{Ru}$ g$_{Support}^{-1}$; 40 mol$_{MOH}$ mol$_{Ru}^{-1}$ (white bars, uniform amount of hydroxide); 10 wt% MOH-loading (filled bars, uniform mass of hydroxide); Aluminum oxide support material 1.0 mm Ø.

catalytic activity and CO_2 selectivity was monitored over prolonged time on stream as depicted for KOH and CsOH coated Ru-**3**-SLP catalysts in Figure 2. Compared to the previously reported KOH-based SLP catalyst, the activity was now almost twice as high (29 h^{-1} vs. initial 14 h^{-1}) due to better handling of the catalyst and removal of dissolved oxygen from both methanol and water. The CO_2 selectivity of >99.9% corresponded to 250 ppm CO in the product gas mixture. The value would not allow direct use in low temperature PEM fuel cells, however, established HT-PEMFC could be operated with this gas stream.[16] As can be seen from Figure 2, the activity of the KOH coated Ru-**3**-SLP catalyst declined over time on stream. As deactivation rate we defined the loss of activity in % per h, resulting in a value of 0.4% h^{-1} for KOH. The second data set included in Figure 3 represents the same Ru-SLP catalyst with CsOH as hydroxide coating. As can be seen, this catalyst showed a marginally lower activity at 23 h^{-1}, while maintaining a constant activity. The selectivity towards CO_2 is comparable to the SLP with KOH coating at 99.8%.

To investigate the effect of the nature of hydroxide on the catalytic performance further, Ru-**3**-SLP catalysts were prepared with different hydroxide coatings, including LiOH, NaOH, CsOH and RbOH. Since the density of these hydroxides varied significantly, we prepared one set of SLP materials with a constant weight loading of 10 wt% hydroxide, while the other set was prepared with a constant molar ratio of hydroxide to Ru-complex **3** of 40.

Of all hydroxides tested, CsOH yielded far more active Ru-**3**-SLP catalysts with peak performances of 50 h^{-1}, while LiOH and NaOH led to rather low activities. RbOH mshowed comparable activity to the KOH system. This increase in activity in order of Li < Na < K < Rb < Cs can on the one hand be attributed to the increased base strength. The selectivity towards CO_2 ranged from 99.5 to 99.8% for the different hydroxides, with no discernable difference between the investigated bases (see Figure S3 in the Supporting Information). Multiple studies have shown the vital role of the base in the catalytic cycle of the Ru-pincer complex, therefore a higher concentration of hydroxide ions could lead to a more active catalyst. Indeed, the activity values correlated with the pK_B values of the various hydroxides as shown in Table 1.

On the other hand, the solubility of water and methanol in the basic coating is important for the catalyst performance. The hygroscopic nature of the salt leads to an absorption of vapors into the coating and reduces the melting point of the salt to appropriate levels. With increasing solubility and subsequently higher hygroscopy a higher concentration of substrates is available for the catalyst. Again, the activity values increased with increasing hygroscopy. Most likely a combination of both factors, pK_B and hygroscopic nature, is crucial for achieving the best performance.

Because of the different densities and molar masses of the metal hydroxides the dry pore filling degrees of the SLP

Table 1. Selected physical parameters of used basic additives for Ru-**3**-SLP catalysts and corresponding TOF of SLP catalyst. pK_B data taken from.[28]

Hydroxide	TOF [h^{-1}][a]	pK_B	S_{water} [g L^{-1}][b]	Density [g L^{-1}][c]
LiOH	4.5	0.18	128	1.5
NaOH	8.4	−0.56	1090	2.1
KOH	29.4	−1.10	1130	2.0
RbOH	29.7	−1.40	1800	3.0
CsOH	50.2	−1.76	3000	3.7

[a] TOF = turnover frequency. [b] Solubility of hydroxide in water at room temperature. [c] Dry density of hydroxide.

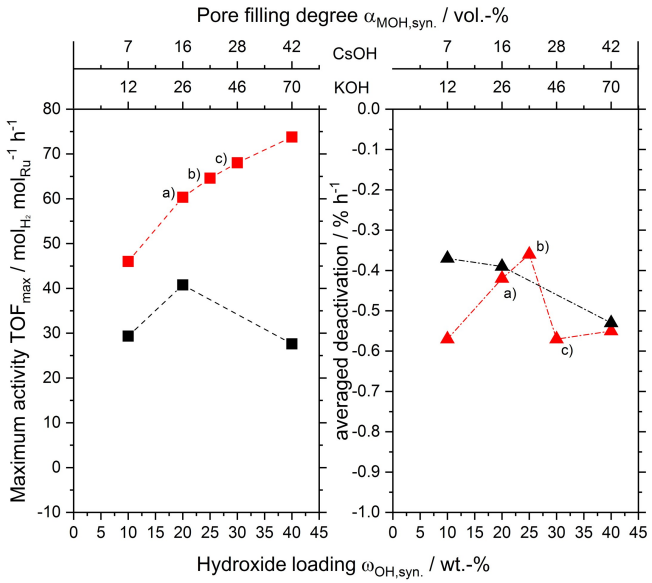

Figure 4. Methanol reforming using Ru-**3**-SLP catalysts with different loadings of KOH (black) and CsOH (red) hydroxides. Activity (squares, left) and averaged change in activity (triangles, right) of immobilized Ru-Pincer-based SLP catalysts in continuous methanol reforming. Average values of a) 8, b) 3 and c) 4 measurements are shown for CsOH. Reaction conditions: T = 150 °C, p_{abs}: 1 bar; $p_{MeOH|H2O}$: 0.5 bar; m_{SLP}: 5.0–6.5 g; Q_{tot}: 50 ml min^{-1}. Catalyst composition: 50 μmol_{Ru} $g_{Support}^{-1}$; Aluminum oxide support material 1.0 mm Ø.

catalysts vary vastly. While for LiOH, NaOH, KOH and RbOH the diverging pore filling degrees showed only minor impact on the activity of the SLP catalyst, the difference in CsOH loading more than doubled the TOF of the catalyst from 23 to 50 h^{-1} (see Figure 3). Therefore, the pore filling degree was investigated in more detail. Figure 4 compares the activity and stability (shown as average change in activity) over different loadings of either KOH or CsOH.

The values of the pore filling can only be determined based on the synthesis protocol. The real pore filling degree at reaction conditions was most likely far higher due to film swelling from dissolved water and methanol. The Ru-**3**-SLP catalyst with KOH coating showed only a minor dependency of its activity upon changing the base loading. Merely a 30% improvement was achieved when increasing the pore filling from 12 to 26 vol%. This is also consistent to previously published investigations using the same Ru-**3**-SLP system.[27] Higher loading beyond 26 vol% resulted in a declined activity, most likely due to pore blocking by the now strongly swollen hydroxide film. Simultaneously, the stability dropped with increasing hydroxide loading, which might hint an elevated leaching of active material from fully liquid-filled pores. On the contrary when employing CsOH as a coating material an increase from 7 to 42 vol% pore filling consecutively led to more active catalysts. The TOF seemed to follow an asymptotic trend without a distinct maximum. At the same time the most stable catalyst was achieved with a CsOH pore filling degree of around 20 vol%. Hence, a compromise between activity and long-term stability has to be accepted.

In line with the recently reported bi-catalytic system in liquid phase methanol reforming we adapted our Ru-SLP catalyst accordingly. By employing a SLP system consisting of the two different Ru-pincer complexes **3** and **5** in a 1:1 ratio, the TOF in gas-phase methanol reforming could be increased from 35 h^{-1} (pure Ru-**3**-SLP) to 85 h^{-1}, resembling an increase by 115%. (see Figure 5) The CO_2 selectivity slightly declined with increasing activity of the bi-metallic Ru-**3**-**5**-SLP system. This is in agreement with previous studies from Beller and co-workers of such bi-metallic systems in AMR. When using **5** in excess compared to **3**, both the activity and selectivity declined drastically. While **3** prefers a high pH of 10 and beyond, **5** prefers neutral or slightly acidic conditions. This might also be the reason for the poor performance of pure Ru-**5**-SLP with basic coating. Interestingly, the lowest deactivation of −0.16% h^{-1} is observed for the 1:1 ratio showing highest activity, while pure Ru-**3**-SLP and Ru-**5**-SLP deactivated faster with −0.3 and −0.62% h^{-1}, respectively.

To investigate if the observed beneficial effect of the CsOH coating can be expanded to the bi-catalytic system, a series of Ru-**3**-**5**-SLP catalysts with different ratios of **3:5** with KOH and CsOH as basic additives was studied. As seen in Figure 5, for a 1:1 ratio there was virtually no difference between the KOH and CsOH coating, both having an initial TOF of around 70 h^{-1}. While the activity of the KOH-based Ru-SLP catalyst declined linearly with reduced amount of **5**, the catalyst with CsOH showed a vastly different trend. A distinct activity maximum was found at a 5:1 ratio of **3:5** with a TOF of 91 h^{-1}. Over the whole range the more basic additive CsOH resulted in more active Ru-**3**-**5**-SLP catalysts.

The CO_2 selectivity was neither influenced by the ratio or the hydroxide coating to a large extend, showing a selectivity of > 99.8% (equal to 1250 ppm CO) throughout all experiments.

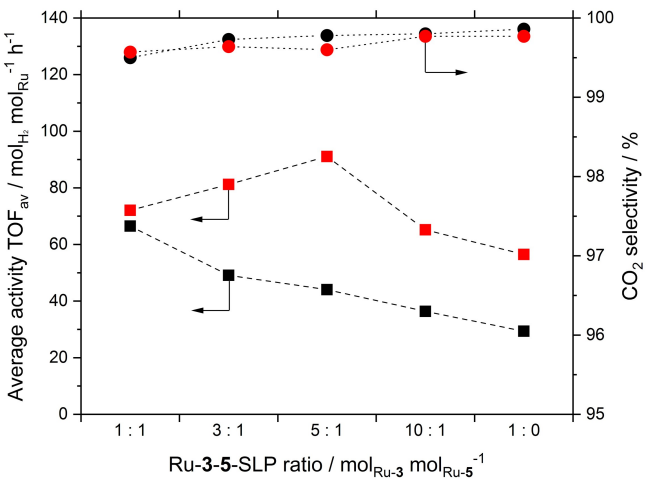

Figure 5. Continuous gas-phase methanol reforming using bi-metallic Ru-**3**-**5**-SLP catalysts with different ratios of **3:5** and varying loadings of KOH (black) and CsOH (red). Activity (squares, TOF) and selectivity towards CO_2 (circles) over time on stream. Reaction conditions: T = 150 °C, p_{abs}: 1 bar; $p_{MeOH|H2O}$: 0.5 bar; m_{SLP}: 5.7 g (CsOH), 5.0 g (KOH), 1.5 g (KOH 1:1); Q_{tot}: 50 ml min^{-1}. Catalyst composition: 50 μmol_{Ru} $g_{Support}^{-1}$; 40 mol_{KOH} mol_{Ru}^{-1}; 10 wt% KOH-loading, 30 mol_{CsOH} mol_{Ru}^{-1}; 20 wt% CsOH-loading; Aluminum oxide support material 1.0 mm Ø.

Table 2. Activity (TOF) and effective activation energy ($E_{A,eff}$) of immobilized, mono- and bi-catalytic Ru-pincer-based SLP catalysts in continuous methanol steam reforming with KOH or CsOH basic additive.[a]

Catalyst	Hydroxide	Temperature [°C]	TOF [h^{-1}]	$E_{A,eff}$ [kJ mol^{-1}]
Ru-**3**-SLP	KOH	120	9	59
		130	14	
		140	23	
		150	34	
		160	48	
Ru-**3**-SLP	CsOH	120	11	68
		130	22	
		140	38	
		150	57	
		160	75	
Ru-**3**-**5**-SLP	KOH	120	21	36
		130	28	
		140	35	
		150	46	
		160	58	
Ru-**3**-**5**-SLP	CsOH	120	23	59
		130	37	
		140	57	
		150	80	
		160	97	

[a] Reaction conditions: p_{abs}: 1 bar; $p_{MeOH|H2O}$: 0.5 bar; m_{SLP}: 5.7 g (CsOH); Q_{tot}: 50 ml min^{-1}; T: 120–160 °C. Catalyst composition: 50 μmol_{Ru} $g_{Support}^{-1}$; 1:1 Ru-**3**-**5**-SLP; 91 mol_{KOH} mol_{Ru}^{-1}; 20 wt% KOH-loading, 31 mol_{CsOH} mol_{Ru}^{-1}; 20 wt% CsOH-loading; Aluminum oxide support material 1.0 mm Ø.

The long-term stability of the different catalysts followed no distinct trend (see Supporting Information for details).

The different trends and correlations between the mono- and bi-catalytic systems, as well as different basic additives can have a plethora of physical or chemical reasons. While the catalytic cycle of the Ru-Pincer complex **3** is strongly dependent on the concentration of hydroxide ions in solution, **5** favors a different pH regime. Additionally the different pK_B values and hygroscopic nature of the metal hydroxides KOH and CsOH lead to different pore filling degrees at reaction conditions and concentrations of reactants in the active film. In Table 2 the four distinct catalytic systems have been investigated over a temperature range of 120–160 °C.

From the set of temperature dependent studies, the effective activation energies could be calculated for the mono-catalytic Ru-**3**-SLP in both hydroxides as well as the bi-catalytic Ru-**3**-**5**-SLP in both hydroxides. Compared to Ru-**3**-SLP, the bi-catalytic system showed a lower $E_{A,eff}$ in both KOH and CsOH, with a stronger decline by 23 kJ mol^{-1} from 59 to 36 kJ mol^{-1} in KOH. The effect is smaller in CsOH, where the effective activation energy is lowered by 9 kJ mol^{-1} only. Since several effects-e. g. pore diffusion, liquid film viscosity, solubility in the liquid mixture – contribute to the effective activation energy in SLP catalysis, no clear insight on molecular level can be made here. In liquid-phase methanol reforming, activation energies of 82 kJ mol^{-1} for complex **3** and 67 kJ mol^{-1} for complex **5** have been determined.[29] While these data do not allow a direct comparison, the range is similar for all systems studied. More detailed kinetic investigations would be mandatory to further elucidate the SLP mechanism at hand.

The influence of both hydroxide and Ru complex on activity is shown in Figure 6 as a function of temperature. The activity at 120 °C with KOH as hydroxide coating was used to normalize the data sets. In doing so, an activity enhancement E_{TOF} as function of hydroxide or catalyst type could be calculated, the results are summarized in Figure 6. The effect of Ru-complex combination in methanol reforming is highlighted by the strong enhancement of up to 1.33 when going from Ru-**3**-SLP to Ru-**3**-**5**-SLP while keeping the KOH hydroxide coating. This 133% increase in activity is observed at lowest temperature of 120 °C. A steep decline in the enhancement is observed when going to higher temperatures, limiting the enhancement to a mere 20% at 160 °C. This is in line with the different activation energies obtained from liquid-phase reforming. The higher activation energy of complex **3** (82 kJ mol^{-1}) leads to higher rate acceleration with increasing temperature. At the same time, the temperature dependency of complex **5** is lower, with only 67 kJ mol^{-1}. Hence, at higher temperatures the catalyst complex **3** is active enough to catalyze all three steps in the MSR cycle effectively and the presence of complex **5** is not really required. This picture is obviously different at lower temperatures, where complex **5** helps to accelerate the final step in the cycle.

The effect of hydroxide is not as strong for activity enhancement, approx. 80% can be obtained at 150 °C for both the Ru-**3**-SLP and the Ru-**3**-**5**-SLP system when changing from KOH to CsOH.

Conclusion and outlook

In the present work we have expanded the investigations on the novel SLP catalyst for methanol steam reforming. Variation of the base showed a strong impact on the overall performance

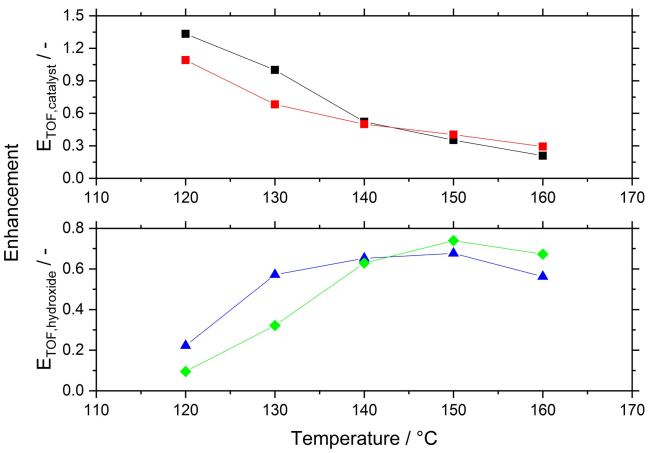

Figure 6. Activity enhancement for Ru-SLP catalysts in gas-phase methanol reforming. Enhancement as a function of catalyst (Ru-3-5-SLP compared to Ru-3-SLP) is shown at the top for both hydroxides KOH (black) and CsOH (red). Enhancement as a function of hydroxide (CsOH compared to KOH) is shown on the right y-axis for both Ru-**3**-SLP (blue) and Ru-**5**-SLP (green). Reaction conditions: p_{abs}: 1 bar; pMeOH | H_2O: 0.5 bar; m_{SLP}: 5.7 g (CsOH); Q_{tot}: 50 ml min^{-1}; T: 120–160 °C. Catalyst composition: 50 μmol_{Ru} $g_{Support}^{-1}$; 91 mol_{KOH} mol_{Ru}^{-1}; 20 wt% KOH-loading, 31 mol_{CsOH} mol_{Ru}^{-1}; 20 wt% CsOH-loading; Aluminum oxide support material 1.0 mm Ø.

of the catalyst. KOH and CsOH were identified as most promising basic additives and coating materials. Peak performances of 41 h^{-1} (SLP with KOH) and 74 h^{-1} (SLP with CsOH) could be achieved at optimized pore filling degrees. Additionally, a bi-catalytic system, consisting of two distinct Ru-pincer complexes was employed to further enhance the activity and long-term stability of the SLP catalysts. A TOF of 91 h^{-1} was achieved with this optimized bi-catalytic SLP catalyst with CsOH coating, which is a threefold improvement of TOF compared to our recent results at comparable reaction conditions.

Experimental Section

All syntheses of Ru-SLP catalysts were carried out under an inert atmosphere of Ar (99.999 vol%, Air Liquide) using standard Schlenk techniques. The carbonylchlorohydrido [bis(2-di-i- propylphosphinoethyl)amine]ruthenium(II) complex **3** was purchased from Strem Chemicals and stored in a glovebox (Vacuum Atmosphere Company, OMNI-LAB) prior to use. The complex **5** was prepared at LIKAT according to a literature procedure.[30] It was shipped in a sealed ampule and stored at FAU in a glovebox prior to use.

Synthesis of supported Ru-pincer catalysts

For the impregnation of the support materials the homogeneous Ru-complex, powdery LiOH (Acros Organics; CAS 1310-65-2), NaOH (Alfa Aesar; CAS 1310-73-2), $RbOH{\cdot}H_2O$ (Alfa Aesar; CAS 12026-05-0), $CsOH{\cdot}H_2O$ (Alfa Aesar; CAS 35103-79-8) and KOH (Merck; CAS 1310-58-3) were dissolved in methanol (LC-MS grade; VWR CAS: 67-56-1) and stirred for at least an hour. Next, the aluminum oxide support material (Sasol Germany, alumina spheres 1.0/160, 1.06 mm average particle diameter, 163 $m^2 g^{-1}$ specific surface area) was added and dispersed in the solution for approx. 10 minutes in order to avoid mechanical stress on the support. The solvent was then slowly removed under reduced pressure in a rotary evaporator to facilitate homogeneous coating of the support material. Afterwards, the optically dry catalyst was again evacuated at <10 mbar for half an hour and stored under argon atmosphere prior to use. Solid substances have been dried, and liquids have been degassed prior to use.

Characterization of the supported molecular catalysts

The content of active metals and other elements, and their ratio, was determined by inductively coupled plasma-atom emission spectroscopy (ICP-AES) using a Ciros CCD (Spectro Analytical Instruments GmbH). The solid samples were digested with concentrated HCl:HNO_3:HF in a 3:1:1 ratio in volume, using microwave heating up to 220 °C for 40 min. (CAUTION: HF is extremely harmful, relevant safety precautions must be taken). The instrument was calibrated with standard solutions of the relevant elements prior to the measurements.

Continuous gas-phase reactor setup

The continuous vapor phase methanol steam reforming experiments were conducted using a fixed bed reactor setup. A simplified flow scheme is shown in Figure 7, for a detailed flow scheme see Figures S1 and S2 in the Supporting Information. The liquid substrates methanol and bi-distilled water were delivered via two independent mass flow controllers (Liqui-Flow; Bronkhorst) into a heating coil followed by an evaporating column in order to minimize pulsations. No inert gas as diluting or balancing agent was applied in the reactor.

Nitrogen (99.9990 vol%, Linde Gas) was used for starting up and shutting down the reactor in order to avoid condensation and was supplied and regulated by a mass flow controller (El-Flow; Bronkhorst). Furthermore, in order to achieve reasonable resolution concerning measurement times, the product gas was diluted after the reactor with a defined N_2 stream (F_{N2}, typically 200 $mL_N min^{-1}$). The gaseous compounds were dried over silica beds, quantified by a mass flow meter (El-Flow; Bronkhorst) and analyzed by an on-line IR- and TCD-based Gas Analyzer (X-Stream Enhanced; Emerson). The hydrogen flow at the reactor outlet F_{H2} was calculated according to Equation (1), taking into account the measured volume flow $F_{H2,out}$ of the effluent gas, the correction factors for the respective compounds K_{H2} and temperature T_{corr} as well as the volume fraction x_{H2}.

$$F_{H2} = F_{H2,out} \cdot x_{H2} \cdot K_{H2} \cdot T_{corr} \quad (1)$$

The maximum product flow $F_{H2,max}$, based on the inlet composition, was calculated according to Equation (2), taking into account the stoichiometry. The mass flow of methanol $\dot{m}_{MeOH}$was additionally checked by taking samples from the condensate from time to time.

$$F_{H2,max} = 3 \cdot \frac{\dot{m}_{MeOH}}{M_{MeOH}} \cdot v_{H2} + 3 \cdot \frac{\dot{m}_{MeOH}}{M_{MeOH}} \cdot v_{CO2} \quad (2)$$

From these two flows, the conversion with respect to methanol was calculated.

$$X_{MeOH} = \frac{F_{H2,out}}{F_{H2,max}} \quad (3)$$

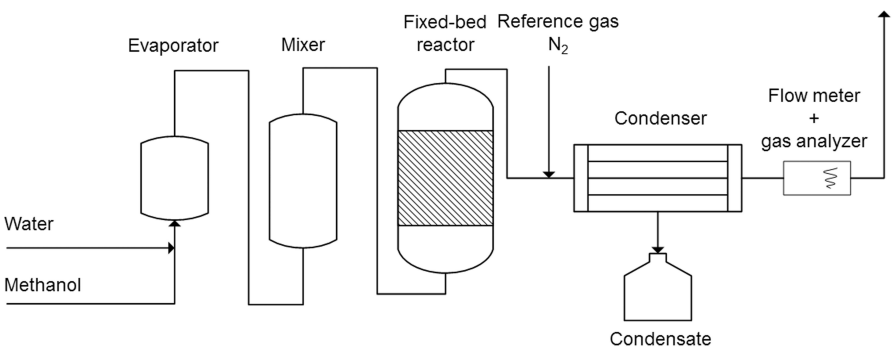

Figure 7. Simplified flow scheme of the continuous vapor phase methanol steam reforming setup.

The selectivity towards CO_2 was calculated from the gas analyzer data directly according to Equation (4). No hints of other carbonaceous compounds were found in random samples.

$$S_{CO2} = \frac{x_{CO2}}{x_{CO2} + x_{CO}} \quad (4)$$

The activity of the Ru-SLP catalysts was assigned by means of turn over frequency TOF, taking into account the known number of moles of Ru n_{Ru} inside the SLP catalyst.

$$TOF = \frac{F_{H2,out}}{\nu_{H2} \cdot n_{Ru}} \quad (5)$$

The activity enhancement by either hydroxide coating or nature of the catalyst was calculated by normalizing the TOF to the standard one obtained for Ru-**3**-SLP with KOH coating at 120 °C.

$$E_{TOF} = \frac{TOF}{TOF_{std}} = \frac{TOF}{TOF_{Ru-3-SLP,KOH,120°C}} \quad (6)$$

Acknowledgements

The authors gratefully acknowledge funding from the German Federal Ministry of Economic Affairs and Energy (BMWi) within the project Metha-Cycle (grant number 03ET6071F). Open access funding enabled and organized by Projekt DEAL.

Conflict of Interest

The authors declare no conflict of interest.

Keywords: Methanol reforming · Ru-pincer catalyst · Supported liquid phase · Immobilization · Alkali hydroxide

[1] G. A. Olah, G. K. Prakash, A. Goeppert, *J. Am. Chem. Soc.* **2011**, *133*, 12881–12898.
[2] P. Makowski, A. Thomas, P. Kuhn, F. Goettmann, *Energ. Environm. Sci.* **2009**, *2*, 480–490.
[3] K. Zeng, D. Zhang, *Progr. Energ. Comb. Sci.* **2010**, *36*, 307–326.
[4] M. Carmo, D. L. Fritz, J. Mergel, D. Stolten, *Int. J. Hydrogen Energy* **2013**, *38*, 4901–4934.
[5] K. Müller, W. Arlt, *Energ. Tech.* **2013**, *1*, 501–511.
[6] D. Teichmann, W. Arlt, P. Wasserscheid, *Int. J. Hydrogen Energy* **2012**, *37*, 18118–18132.
[7] P. Preuster, C. Papp, P. Wasserscheid, *Acc. Chem. Res.* **2017**, *50*, 74–85.
[8] P. Preuster, A. Alekseev, P. Wasserscheid, *Annu. Rev. Chem. Biomol. Eng.* **2017**, *8*, 445–471.
[9] P. M. Modisha, C. N. M. Ouma, R. Garidzirai, P. Wasserscheid, D. Bessarabov, *Energ. Fuels* **2019**, *33*, 2778–2796.
[10] Y. Okada, E. Sasaki, E. Watanabe, S. Hyodo, H. Nishijima, *Int. J. Hydrogen Energy* **2006**, *31*, 1348–1355.
[11] Y. Shen, Y. Zhan, S. Li, F. Ning, Y. Du, Y. Huang, T. He, X. Zhou, *Chem. Sci.* **2017**, *8*, 7498–7504.
[12] B. Loges, A. Boddien, H. Junge, M. Beller, *Angew. Chem. Int. Ed.* **2008**, *47*, 3962–3965; *Angew. Chem.* **2008**, *120*, 4026–4029.
[13] K. Sordakis, C. Tang, L. K. Vogt, H. Junge, P. J. Dyson, M. Beller, G. Laurenczy, *Chem. Rev.* **2018**, *118*, 372–433.
[14] G. A. Olah, A. Goeppert, G. K. Surya Prakash, in *Beyond Oil and Gas: The Methanol Economy* (Eds.: G. A. Olah, A. Goeppert, G. K. Surya Prakash), Wiley-VCH, Weinheim, **2018**.
[15] A. Iulianelli, P. Ribeirinha, A. Mendes, A. Basile, *Renewable Sustainable Energy Rev.* **2014**, *29*, 355–368.
[16] A. L. Dicks, D. A. J. Rand, *Fuel Cell Systems Explained*, Wiley-VCH, Weinheim, **2018**.
[17] D. R. Palo, R. A. Dagle, J. D. Holladay, *Chem. Rev.* **2007**, *107*, 3992–4021.
[18] S. Sá, H. Silva, L. Brandão, J. M. Sousa, A. Mendes, *Appl. Catal. B* **2010**, *99*, 43–57.
[19] E. Alberico, M. Nielsen, *Chem. Commun.* **2015**, *51*, 6714–6725.
[20] N. Onishi, G. Laurenczy, M. Beller, Y. Himeda, *Coord. Chem. Rev.* **2018**, *373*, 317–332.
[21] J. Kothandaraman, S. Kar, A. Goeppert, R. Sen, G. K. Surya Prakash, *Top. Catal.* **2018**, *61*, 542–559.
[22] P. Hu, Y. Diskin-Posner, Y. Ben-David, D. Milstein, *ACS Catal.* **2014**, *4*, 2649–2652.
[23] A. Mukherjee, D. Milstein, *ACS Catal.* **2018**, *8*, 11435–11469.
[24] a) M. Nielsen, E. Alberico, W. Baumann, H.-J. Drexler, H. Junge, S. Gladiali, M. Beller, *Nature* **2013**, *495*, 85–89; b) E. Alberico, A. J. J. Lennox, L. K. Vogt, H. Jiao, W. Baumann, H.-J. Drexler, M. Nielsen, A. Spannenberg, M. P. Chercinski, H. Junge, M. Beller, *J. Am. Chem. Soc.* **2016**, *138*, 14890–14904.
[25] V. Strobel, J. J. Schuster, A. S. Braeuer, L. K. Vogt, H. Junge, M. Haumann, *React. Chem. Eng.* **2017**, *2*, 390–396.
[26] A. Agapova, H. Junge, M. Beller *Chem. Eur. J.* **2019**, *25*, 9345–9349.
[27] C. H. Schwarz, A. Agapova, H. Junge, M. Haumann, *Catal. Today* **2020**, *342*, 178–186.
[28] http://www.periodensystem-online.de/ (accessed December 2020).
[29] A. Agapova, E. Alberico, A. Kammer, H. Junge, M. Beller, *ChemCatChem* **2019**, *11*, 1910–1914.
[30] Supporting Information of.[24b].

Manuscript received: January 18, 2021
Revised manuscript received: March 8, 2021